Original Research Article

High product yield synthesis of nitrogen doped carbon dots through exothermic reaction for temperature sensing and tartrazine detection

ABSTRACT

Rapid, green and high yield synthesis of nitrogen doped carbon dots(N-CDs) through exothermic decomposition reaction of H_2O_2 using grasshopper powder as precursor and polyethyleneimine (PEI) as a surface passivation reagent. Water-soluble fluorescent N-CDs can be obtained by reacting 5 minutes and purified N-CDs were obtained after an activated carbon adsorption separation procedure with a product yield of 53.3%. TEM, FT-IR, XPS, fluorescence and UV-vis spectra were used to investigate the morphology, elemental information and optical properties of N-CDs. The results indicated that the fluorescence emission of N-CDs is typical excitation wavelength dependent with a strongest emission peak at 417 nm under 330 nm excitation wavelength. There is a good linear response between the fluorescence intensity of N-CDs and temperature, which makes N-CDs a potential nanothermometer to monitor temperature. The great spectral overlap between the blue emission peak (417 nm) of N-CDs and the absorption peak (430 nm) of tartrazine (TAR) leads to an effectively fluorescence quenching phenomenon by TAR through inner filter effect (IFE) and the fluorescence quenching degree (lg(I0/I)) was linearly response to the TAR concentration in the range of 1-100 μM. The detection limit of developed method is 54.3 nM for TAR, and the relative standard deviation (RSD) is 1.14% (n=7, c=10 μM). The N-CDs came from an exothermic reaction is a highly selective and sensitive fluorescent probe for TAR, and it was successfully applied to the determination of TAR in food samples with satisfactory results.

Keywords: Tartrazine, Carbon dots, Inner filter effect, Food samples, Exothermic reaction

1. INTRODUCTION

Tartrazine (TAR, $C_{16}H_9N_4Na_3O_9S_2$, E102) is a yellow-color synthetic colorant and widely used as food additive in various food products, such as cookies, soft drinks, candies, jelly and energy drink[1, 2]. Unfortunately, studies have reported that excessive TAR may be associated with thyroid tumors, chromosomal damage, allergies, asthma, urticaria and overactive behavior in children[3-5]. Hence, TAR adding in food products is strictly controlled based on admissible daily intake (ADI) values. The ADI of TAR is recommended to be 7.5 mg kg^{-1} bw/day by Joint FAO/WHO Expert Committee and EU Scientific Committee for Food (SCF)[6]. Therefore, it is particularly important to develop simple, selective, sensitive methods for monitoring the amount of TAR in different food matrices.

Now, many analytical methods have been applied for the determination of TAR in food samples including HPLC[7, 8], LC-MS[9, 10], spectrophotometry[11], electrochemical methods[12, 13], however, these methods require expensive and specialized instruments, harsh working conditions, long analytical time, complicated sample preparation, which limits their applications in routine monitoring of TAR in food matrices[14, 15]. Recently, Carbon dots (CDs) based fluorescence sensors for food safety monitoring have attracted more and more attention due to excellent characteristics of CDs, such as excellent water solubility, low toxicity, tunable emission, and stability against photobleaching[16-18]. A series of CDs were prepared for fluorescence sensing of TAR with good analytical performances[19-28]. However, hydrothermal procedure is still the most popular means of obtaining CDs with

excellent optical properties, which is a time-consuming, energy-consuming preparation method, often accompanied by a longer dialysis purification process. Even with these violent preparation methods, the product yield (PY) of CDs is still at a very low level[29]. Therefore, exploring rapid and green method for preparing CDs with high PY is in great need.

In this work, grasshopper powder was chosen as carbon source, and PEI was used as surface passivation reagent; a large amount of heat released by decomposition reaction of H_2O_2 under alkaline condition is used as heat source to realize the generation of CDs and doping of N element. The obtained N-CDs solution was purified by an activated carbon adsorption process to remove excess raw materials and byproducts. The calculated QY for N-CDs based on the mass of obtained N-CDs solid powder and raw materials is 55.3%. Scheme 1 demonstrated the preparation strategy of N-CDs and the sensing principle for TAR. The absorption spectrum of TAR largely overlaps with the fluorescence emission spectrum of N-CDs, which leads to a fluorescence quenching of N-CDs by the presence of TAR in solutions through IFE mechanism. Based on IFE mechanism, a new TAR fluorescence assay was developed. The analytical results of real food samples proved that the assay possess the characteristics of high sensitivity, selectivity, rapidity and low cost.

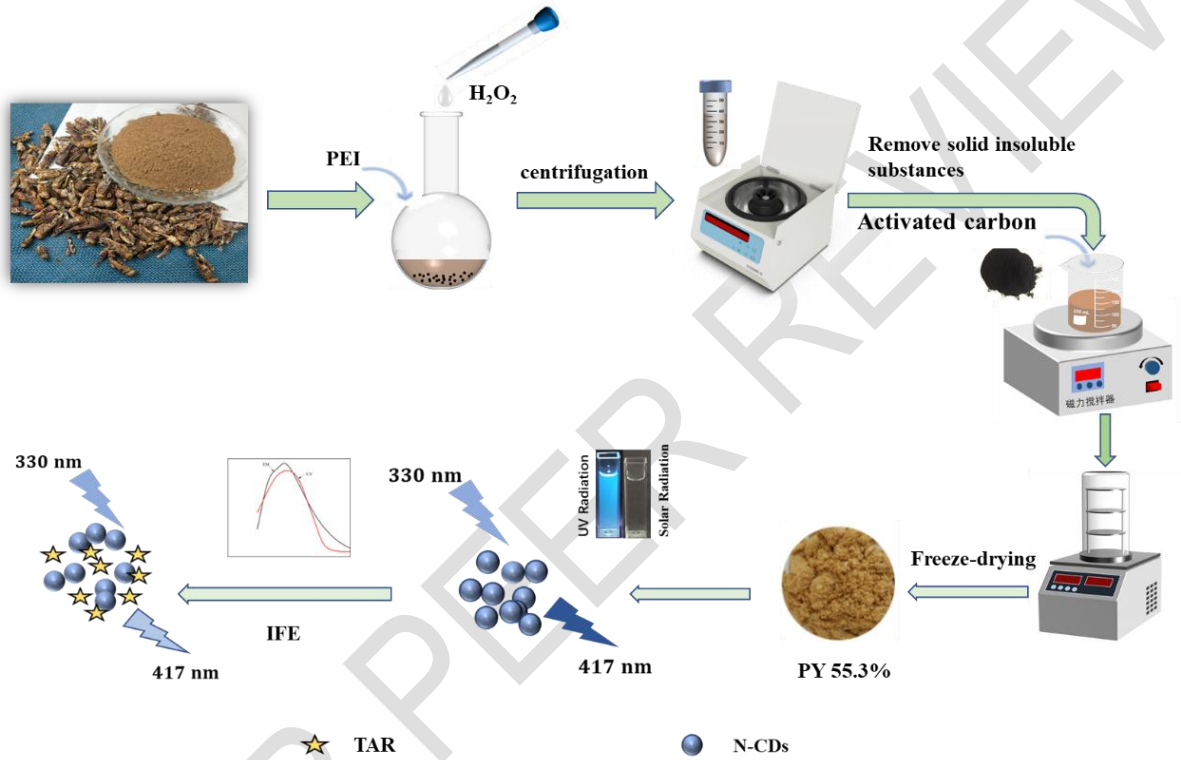

Scheme 1 A schematic diagram of the preparation strategy of N-CDs and the sensing principles for TAR

2. EXPERIMENTAL DETAILS

2.1 Apparatus and Reagents

The morphology and elemental composition information of N-CDs were obtained by TEM (JEM-2011, Japan), XPS (Thermo Escalab 250Xi, USA) and FT-IR (WQF-530, Beijing Beifen-Ruili Analytical Instrument (Group) Co. Ltd., Beijing, China). Fluorescence spectrometers (Shimadzu, Japan, F-6000; Horiba Jobin Yvon, France) were employed to collect fluorescence emission spectra and fluorescence lifetime of N-CDs. And the Absorption curves were recorded on a UV-2450 spectrophotometer (Shimadzu).

TAR, H_2O_2, and polyethyleneimine (M.W. 600, PEI) were provided by Sangon Biotech (Shanghai) Co. Ltd (Shanghai, China). Methionine (Met), glutamate (Glu), lactulose (Lac), glycine (Gly), sucrose (Suc), fructose (Fru), glucose (Glc), Sodium benzoate (SB), citric acid (CA) and nitrite of metals were provided by Aladdin (Shanghai, China). Britton-Robinson (BR) buffer solutions were used to adjusting the acidity of testing solution. Grasshoppers were obtained from School of Food Science and Engineering in Henan University of Technology. Deionized water (18 MΩ·cm) was used throughout the experiments.

2.2 Synthesis of N-CDs

N-CDs derived from grasshopper were fabricated through an exothermic decomposition reaction of in alkaline medium using PEI (M.W. 600) as N dopant. The preparation procedure was modified according to our precious work[30, 31]. Grasshopper powder (1.0 g) was mixed with PEI (100 mg mL^{-1}, 5 mL) in a round flask. Then, H_2O_2 (7 mL, 30%) was dropped to the mixture. With the drip of H_2O_2, due to the rapid decomposition reaction of H_2O_2 under alkaline medium, a large number of bubbles are immediately produced, accompanied by the release of a large amount of heat. The temperature of reaction solution reaches 100 °C within one minute. After 5 minutes, there are no more bubbles in the mixture and the exothermic reaction stopped. After the temperature of the solution dropped to room temperature, deionized water (50 mL) was added to dissolve the produced N-CDs. After removal of solid insoluble substances by centrifugation (8000 r min^{-1},15 min), activated carbon (2.0 g) was mixed with the obtained brown solution and magnetically stirred for 1.0 h. Then the activated carbon adsorbed of impurities were separated by centrifugation, the color of the solution changed from brown to light yellow, indicating that some colored substances in the solution were removed by activated carbon adsorption. The earth-yellow N-CDs powder (0.8 g) was obtained by freeze drying of the purified solution. and was redispersed in deionized water (16 mg mL^{-1}) for the subsequent fluorescence tests.

2.3 Sample preparation

Food samples (Candies, carbonated beverages, bread, rice crust and chicken flavor block) were purchased from Wal-Mart Supermarket (Zhengzhou, China). TAR in solid samples was extracted through a conventional liquid extraction procedure. Each solid sample (5.0 g) was soaked in 25 mL BR (pH 6) buffer solution for 24 h. The sample solutions for test were obtained after a centrifugation separation. The carbonated beverages were heated in a 40 ℃ water bath for 30 min to remove CO_2, and then diluted to a desired volume for subsequent testing.

2.4 Analytical procedure for TAR

N-CDs solution (500 μL), BR buffer (1 mL, pH 9.0) and a certain volume of TAR standard stock solution (or sample solution) were placed in turn to a series of calibrated tubes, the solution was then diluted with deionized water to the desired volume. The fluorescence intensities (417 nm) for the solutions were measured using the excitation wavelength of 330 nm. $lg(I_0/I)$ was calculated, and the standard curve was plotted by $lg(I_0/I)$ against concentrations of TAR, here I and I0 refer to the fluorescence intensities of the sensing solutions with and without TAR, respectively. All experiments are carried with three parallel experiments.

3. RESULTS AND DISCUSSION

3.1 Characterization of N-CDs

HRTEM, FT-IR, XPS, absorption and fluorescence spectroscopy were used to investigated the morphology, elemental information and optical properties of N-CDs from exothermic reaction. Fig. 1a indicates that the average particle size of N-CDs is 5.09±0.37 nm. Calculated lattice fringe spacing is 0.204 nm (inset in Fig. 1b), which may be attributed to the sp^2 (1120) graphitic crystal phase of graphene[32]. The functional groups of N-CDs were confirmed by FT-IR spectrum. As shown in Fig. 1c, the peaks at 3180 cm^{-1} and 779 cm^{-1} are attributed to the stretching vibration peak and the bending vibration peaks of the N-H respectively. The absorption peaks at 1334 cm^{-1} and 1666 cm^{-1} are attributed to the bending vibration peak of C-N and C=C/C=N, respectively. The absorption peaks at 1743cm^{-1} and 3386 cm^{-1} are C=O and O-H stretching vibration peaks[26, 33, 34].

The elemental chemical state of the N-CDs was characterized by XPS. C1s, N1s, and O1s with elemental atomic proportions of 61.8%, 18.1%, and 19.97%, respectively was found in the survey scan of N-CDs. The high-resolution spectrum of C1s (Fig. 1d) shows five peaks at 284.43, 285.46, 286.11, and 287.60 eV, representing the C=C, C-N, C-O, and C=O/C=N groups, respectively. In the high-resolution N1s spectrum (Fig. 1e), the two peaks at 399.57 and 401.79 eV could be assigned to the C-N and N-H groups, respectively. The O1s spectrum (Fig. 1f) shows three fitted peaks at 530.69, 531.23 and 531.94 eV, attributing to the C-O, C-O-H/C-O-C, and C=O groups[19, 35, 36], respectively. In terms of elemental composition information of N-CDs, the results of XPS are consistent with those of FT-IR.

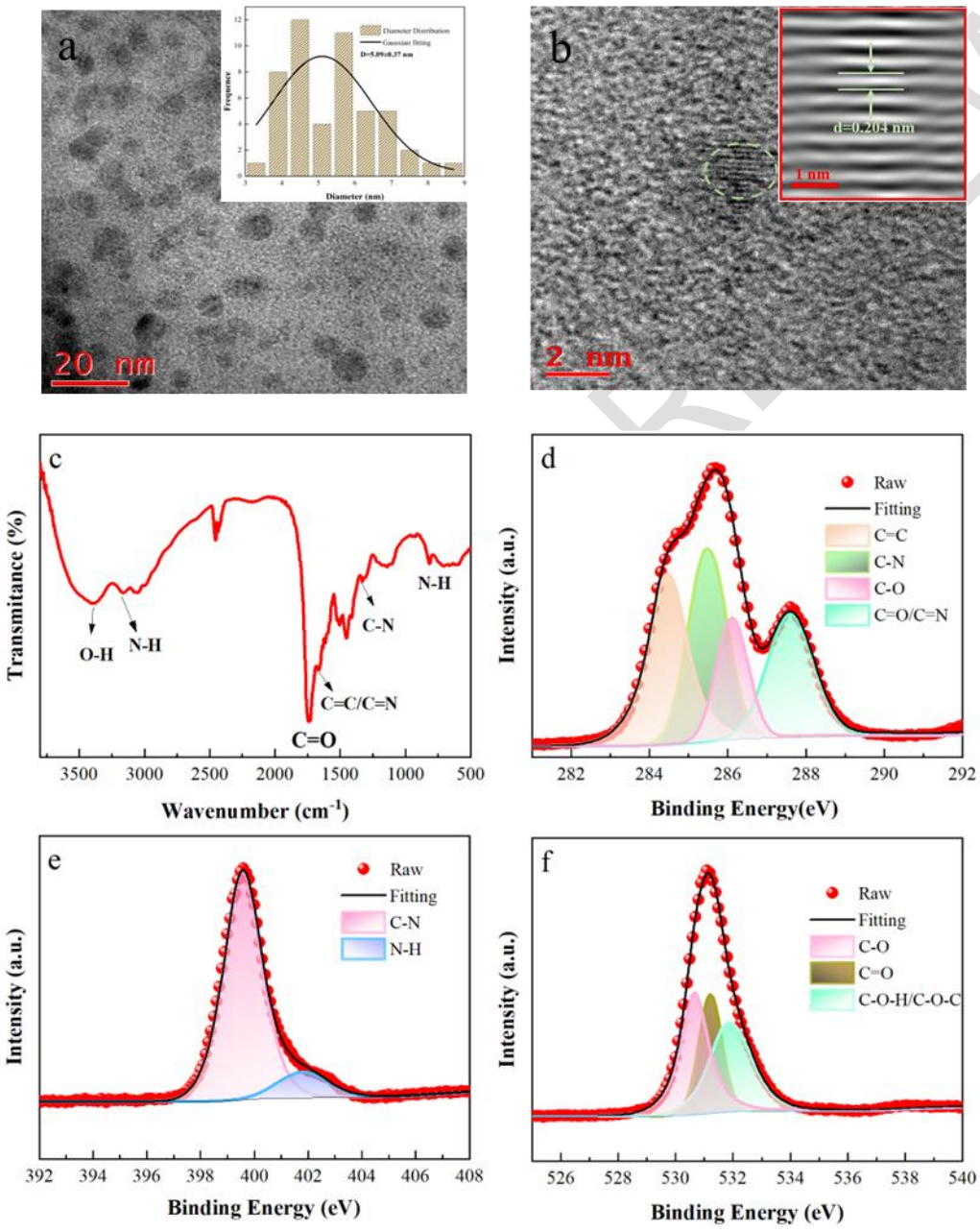

Figure 1. (a) TEM image of the N-CDs. (b) HRTEM image of theN-CDs. (c) FT-IR spectra of the N-CDs. (d) C1s ,(e) N1s and (f) O1s high resolution spectra of the N-CDs.

The optical properties of N-CDs were studied using fluorescence and UV-vis spectroscopy. Two typical UV-vis absorption peaks at 264 nm and 330 nm can be found in absorption curve of N-CDs (Fig.2a). The peak at 264 nm is ascribable to the π-π* transition for the C=C bond, and the absorbance at 330 nm corresponds to the n-π* transition of C=O[37].

In the excitation wavelength range of 290-390 nm, the fluorescence emission behavior of N-CDs showed obvious excitation wavelength dependence (Fig.2b). With the increase of excitation wavelength, the fluorescence emission wavelength is obviously red-shifted, and the fluorescence intensity is gradually enhanced. When the fluorescence intensity reaches the maximum, the fluorescence intensity begins to decrease as the excitation wavelength becomes longer. Under the excitation wavelength of 330 nm, the strongest emission peak of N-CDs is located at 417 nm. The relative fluorescence quantum yield of N-CDs was determined to be about 2 % with quinine sulfate as a reference.

The effects of pH, salt concentration and temperature on the luminescence of N-CDs were studied. It can be seen from Fig.2c that the fluorescence intensity of N-CDs gradually increases with the increase of solution pH values. When pH value is greater than 12, the fluorescence intensity of N-CDs begins to decrease rapidly. This may be explained by the fact that a large number of primary amines, secondary amines groups on the surface of N-CDs are easy to bind H+ under acidic conditions, which changes the surface electronic state of N-CDs, thus affecting the fluorescence emission of N-CDs. Fig.2c showed that even if the salt (NaCl) concentration is as high as 4 M, it still does not have a significant effect on the fluorescence emission of N-CDs, indicating that N-CDs possess excellent salt tolerance property. To study the fluorescence response to the solution temperature variation, the fluorescence spectra of N-CDs were recorded at different temperature ranging from 15 °C -75 °C. At higher temperatures, the fluorescence intensity of N-CDs is lower (Fig.2e). This is due to the activation of non-radiative channels by increasing of temperature, which makes more excited electrons return to the ground state through non-radiative transitions, thus reducing the fluorescence emission of N-CDs[34, 38]. An interesting phenomenon is that the fluorescence intensity of N-CDs also returns to the same initial level when the heated solution is cooled to the same temperature (15 °C). Furthermore, the calculated F/F_0 shows a good linear response to temperature (T, °C) in the temperature range of 15 °C -40 °C and 45°C -75 °C, respectively, where F0 is the fluorescence intensity of N-CDs at 15 °C and F is the fluorescence intensity of N-CDs at other temperatures. Depending on the extraordinary reversible and temperature-sensitive response properties of N-CDs, N-CDs are anticipated to be a potential candidate as a distinguished nanothermometer to monitor temperature.

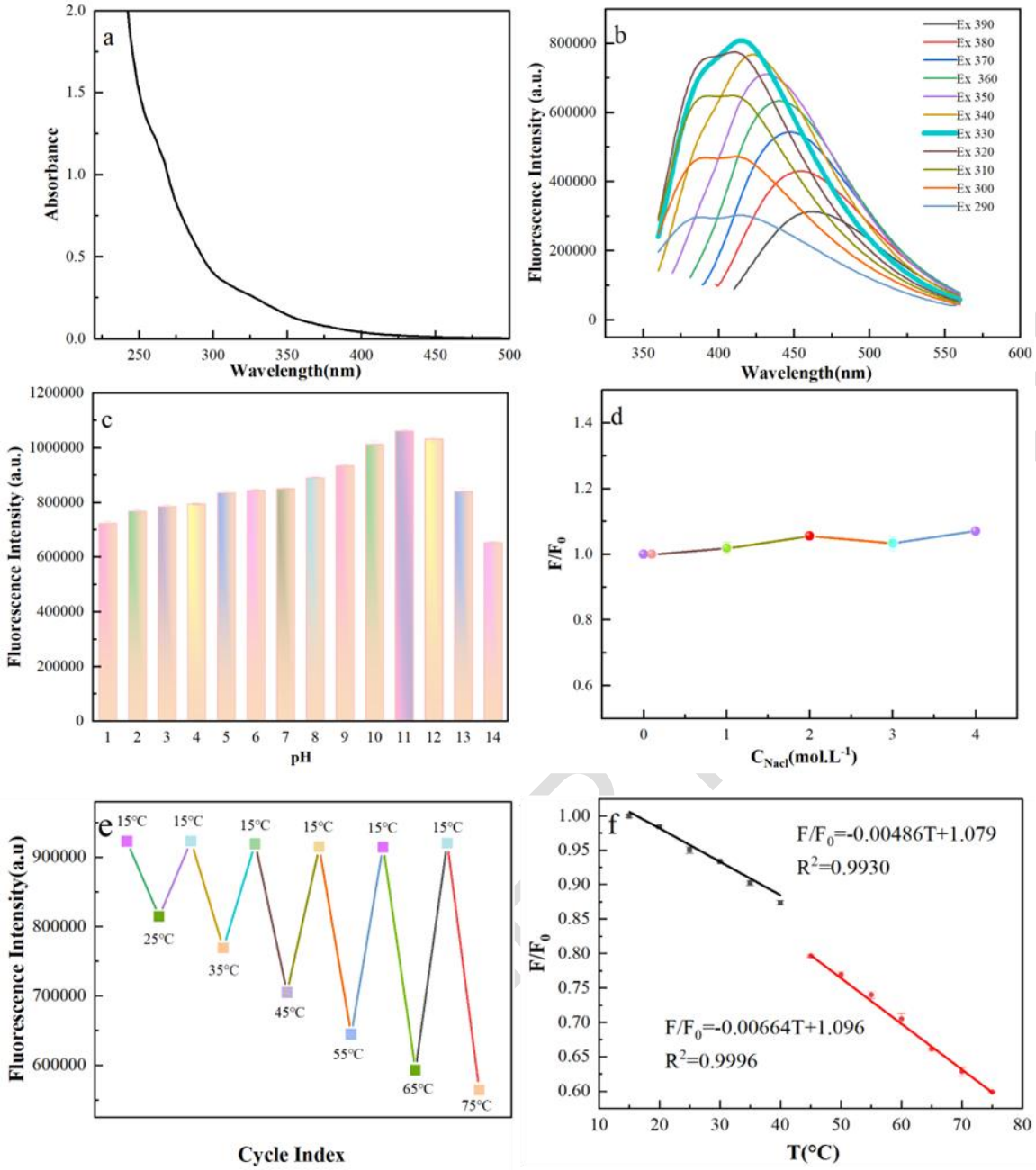

Figure 2. (a) UV-vis absorption spectra of the N-CDs. (b) Fluorescence emission spectra of N-CDs. (c) (Effect of pH on the fluorescence intensity of N-CDs. (d) Effect of NaCl on the fluorescence intensity of N-CDs. (e) Cyclic testing of temperature response with N-CDs. (f) F/F_0 versus temperature plots of N-CDs with temperature range of 15 °C -75 °C.

3.2 Fluorescent sensing of TAR

Because the large spectra overlap between absorption spectrum of TAR and fluorescence emission spectrum of N-CDs, it was found that the fluorescence intensity of N-CDs can be effectively quenched by TAR. The parameters (pH and temperature) affecting the quenching behavior were optimized, and the results were shown in Fig.3. It could be seen from Fig.3a that the quenching efficiency of TAR varies with the change of pH, the maximum quenching efficiency was obtained at pH 9. This is could be explained by the fact that TAR presents different absorption spectra under different pH conditions, which leads to different degree of the spectral overlap with changing pH. Therefore, pH 9 was chosen as the optimal experimental condition. As demonstrated in Figure 3b, in the presence or absence of TAR, the fluorescence intensity of N-CDs decreased with increasing temperature. However, the fluorescence

quenching efficiency of TAR remained almost consistent. The results indicated that temperature had no significant effect on the fluorescence quenching behavior of TAR. Therefore, room temperature was chosen as the best experimental condition.

Under the optimal experimental conditions, the fluorescence spectra of N-CDs with different concentrations of TAR were recorded (Fig.3c). The fluorescence intensities of N-CDs declined gradually with TAR concentration increasing from 0-100 μM. Good linear relationship (R2=0.9993) between the calculated lg(I0/I) and TAR concentration (C, 1-100 μM) was achieved with the linear equation of lg(I0/I)=7907.1C+0.0041 (Fig.3d). The detection limit (3σ) of TAR was estimated to be 54.3 nM, and the relative standard deviation (RSD) is 1.14% (n=7, c=10 μM), which shows that the method has high sensitivity and good repeatability.

Table 1 gives a comparison of the analytical performances of this method with those of CDs-based TAR fluorescent probes reported in the literature. Obviously, the detection limit of this method is comparable to those of reported in the literature. The N-CDs used in this method are rapidly prepared by an exothermic reaction. Compared with the popular hydrothermal method, it not only greatly shortens the reaction time, but also saves a lot of energy.

In addition, compared with the traditional dialysis purification process, the activated carbon adsorption separation method is also more convenient and faster. Of course, compared with filtration using filter membrane, activated carbon adsorption is obviously more efficient for the removal of soluble impurities. Finally, the high PY of this preparation method is also an advantage that should be pointed out. Compared with other preparation methods, 53.3% of PY makes the product obtained from only single preparation sufficient for the whole experiment, which greatly reduces the cost and time of analytical method. Therefore, this method provided a rapid, high PY and low-cost approach to obtain purified N-CDs fluorescent probes, a new TAR sensing method with enough sensitivity for real food samples was developed.

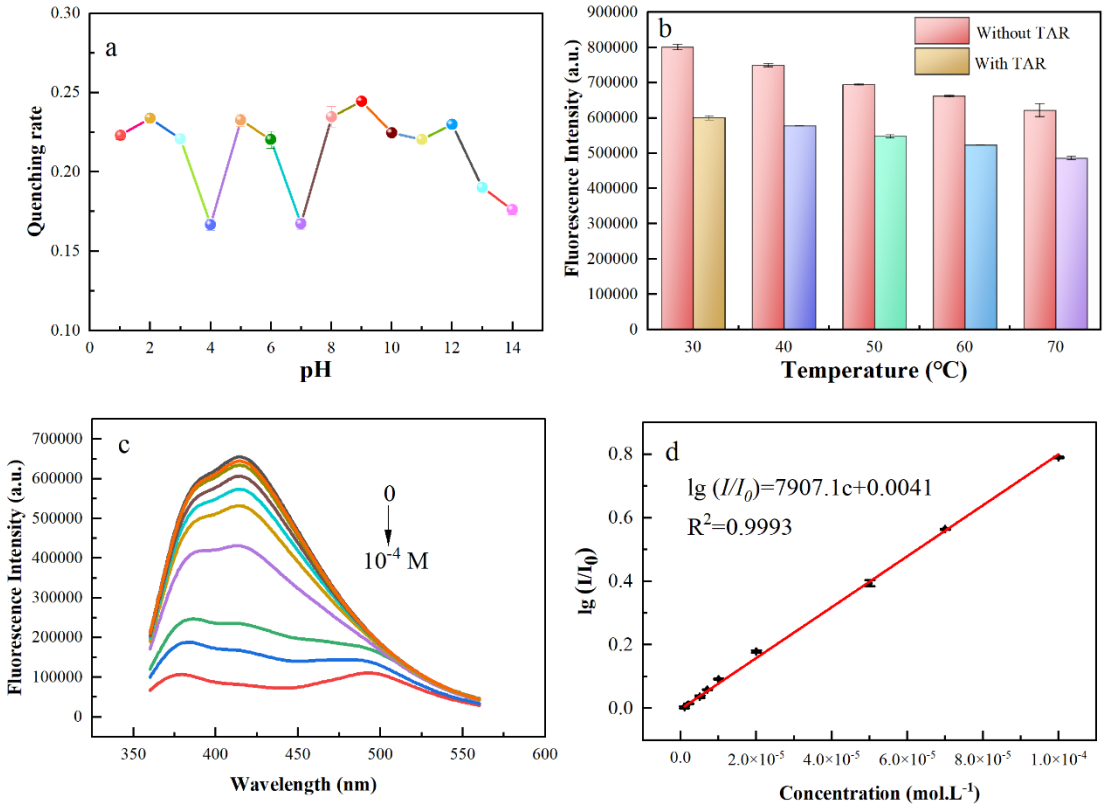

Figure 3. Optimize parameters affecting TAR sensing procedure. (a) pH. (b) temperature. (c) Fluorescence responses of N-CDs in the presence of different concentrations of TAR. (d) Linear relationships between lg(I0/I) and concentration of TAR.

Table 1. Comparison of different CD-based fluorescence methods for detection of TAR

Probes	Synthesis	Purification	Detection limit(nM)	Refs
N, S-CDs	Hydrothermal; 210 °C, 5 h	Filter membrane	80	[20]
N-CDs	Hydrothermal; 180 °C, 4 h	Dialysis tube, 48 h	34.98	[19]
CDs	Hydrothermal; 210 °C, 10 h	Dialysis, 48 h	43.2	[22]
S-CDs	Hydrothermal; 210 °C, 12 h	Dialysis, 4 h	45	[21]
CDs	Hydrothermal; 180 °C, 12 h	Dialysis, 72 h	12.4	[23]
CDs	Hydrothermal; 180 °C, 12 h	Filter membrane	86	[26]
CDs	Hydrothermal; 180 °C, 44 h	Filter membrane, Dialysis, 32 h	26	[25]
N, Cl-CDs	Hydrothermal; 180 °C, 47 h	Filter membrane	48	[24]
CDs	Hydrothermal; 180 °C, 11 h	Filter membrane, CH_2Cl_2 extraction	73	[42]
CDs	Microwave 10 min	-	18	[43]
CDs	Microwave 70 min	Filter membrane	20	[28]
N-CDs	Exothermic reaction, 10 min	Activated carbon adsorption, 0.5 h	54.3	This work

3.3 Selectivity for TC detection

To evaluate the selectivity of the fluorescent sensor for TAR, the influence of possible foreign substances was investigated. For some fluorescent sensors, other ions or organic compounds may interfere with the fluorescence intensity. To accurately measure the TAR concentration in various circumstances, the effects of metal ions and

organic compounds on the fluorescence intensity of N-CDs were examined. As seen in Fig. 4, K^{+}, Zn^{2+}, Na^{+}, Mg^{2+}, Ba^{2+}, Mn^{2+}, Pb^{2+}, Ca^{2+}, Al^{3+}, Fe^{3+} (10 μg mL^{-1}; 1 μg for Ni^{2+},Co^{2+}, and Cr^{6+}) and organic compounds (Met; Glu; Gly; Lac; Fru; Suc, 0.4 M; Glc, 0.8 M; SB, 0.05 M; CA, 0.001 M) each at a concentration of 100 μM had none influence on fluorescence intensity of N-CDs in the presence and absence of TAR, and this indicates the high specificity of the sensor for detecting TAR.

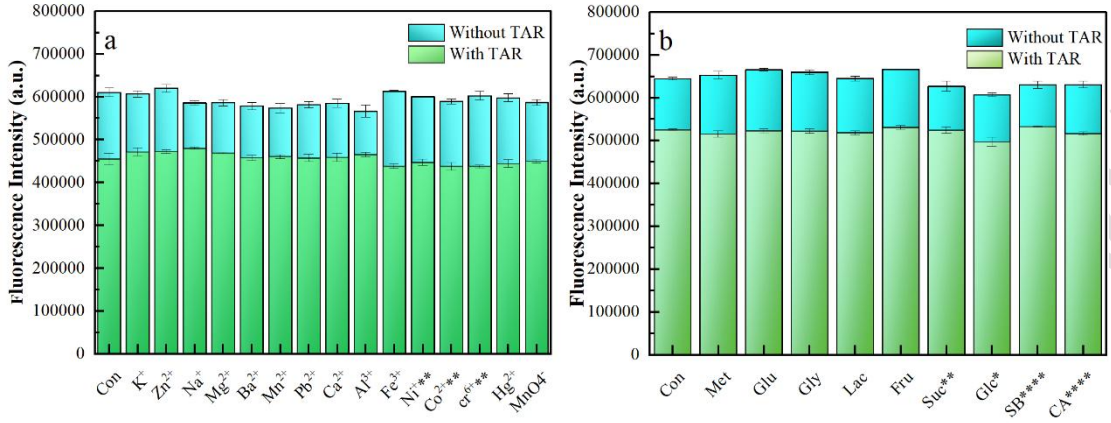

Figure 4. Fluorescence responses of N-CDs to different interfering substances in the absence and presence of TAR (10 μM), interfering metal ions (a, 10 μg mL^{-1}; 1 μg mL^{-1} for ions with *), interfering organic substances (a, 0.4 M; Glc, 0.8 M; SB, 0.05 M; Ca, 0.001 M).

3.4 Fluorescence quenching mechanism

In order to clarify the fluorescence quenching mechanism of N-CDs by TAR, some important parameters were calculated. Firstly, the fluorescence lifetime of N-CDs in presence and absence of TAR was measured. The results showed that the fluorescence lifetime of N-CDs did not change significantly after mixing with TAR (Fig.5a), indicating that quenching mechanism was not dynamic quenching. Then, the quenching rate constant was calculated according to the Stern-Volmer equation. The calculated value (8.7×10^{13} M^{-1} S^{-1}) is much larger than the maximum dynamic quenching rate constant (2.0×10^{10} M^{-1} S^{-1}), which is completely consistent with the results of fluorescence lifetime.

Considering the large spectra overlap between the emission spectrum of N-CDs and the absorption spectrum of TAR (Fig.5b), the fluorescence quenching mechanism may be IFE. According to the mathematical model reported in the literature[39-41], IFE mechanism was verified by calculating the corrected fluorescence intensities of N-CDs. The calculated values showed that the corrected fluorescence intensities of N-CDs mixing with different concentrations of TAR remains almost unchanged, indicating that quenching mechanism is IFE. Finally, the absorption spectrum was used to judge whether there was a complex formation in the mixture of N-CDs and TAR to exclude the possibility of static quenching. The absorption curve of N-CDs-TAR mixing solutions almost coincides with the sum curve of N-CDs and TAR (Fig.5c), which indicated that no N-CDs-TAR complex forms, thus excluding static quenching and confirming IFE.

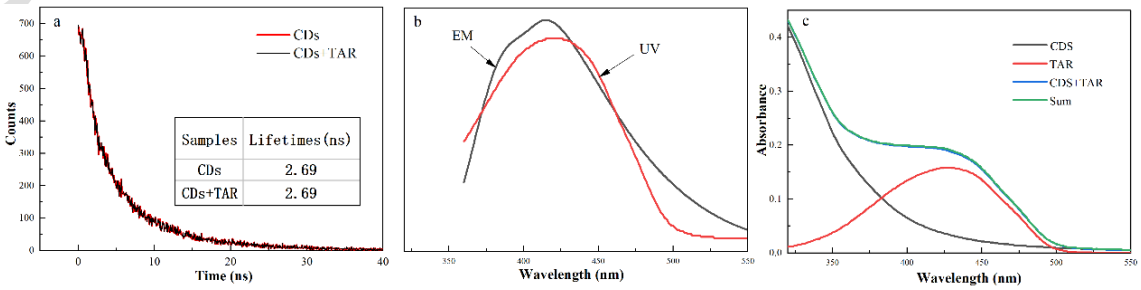

Figure 5. (a) Fluorescence decay curve of N-CDs in the absence and presence of TAR. (b) spectra overlap between

fluorescence emission spectrum of N-CDs and absorption spectrum of TAR. (c) absorption spectra of N-CDs, TAR, N-CDs-TAR mixtures and the sum value of absorptance of N-CDs and TAR

3.5 Determination of TC in real samples

The good feasibility of this method was verified by the analysis of different types of actual food samples. The results of testing and spiking experiments for food samples were listed in Table 2, and the spiked recoveries are between 89.1-120.0%. From these results, it can be concluded that the IFE-based fluorescence assay possesses the advantages of high sensitivity, high accuracy and precision, and is a practical analysis method for artificial pigments in foods.

Table 2. Determination of TAR in food samples (n = 3, mean ± SD, μg g^{-1})

Samples	Added	Found	Recovery (%)
Lollipop	0	21.2±0.60	-
	53	69.7±0.35	91.6%
	106	120.1±0.58	93.3%
Candy corn	0	65.1±2.24	-
	106	163.8±2.57	93.1%
	212	261.6±3.41	92.7%
Carbonated drinks 1	0	7.3±0.02	-
	13.4	19.8±1.09	93.2%
	26.8	33.4±1.97	97.3%
Carbonated drinks 2	0	10.3±0.24	-
	26.7	35.9±3.15	95.9%
	53.4	61.9±2.61	96.6%
Rice crust	0	0	-
	6.7	6.6±0.12	98.5%
	13.4	16.0±1.13	120.0%
Bread	0	5.1±0.45	-
	13.4	18.4±1.52	99.3%
	26.8	29.0±2.12	89.1%
Chicken flavored chunks	0	3.3±0.05	-
	13.4	17.5±1.23	106.0%
	26.8	28.2±1.05	92.9%

4. CONCLUSION

A rapid, facile, low-cost preparation approach for the preparation of N-CDs with high PY was provided. Exothermic reaction was used as the heat source for preparation, and activated carbon adsorption was applied for purification of N-CDs. Both the two processes can be completed within 1 h. The prepared N-CDs served as a

fluorescence probe for TAR with excellent selectivity and sensitivity through IFE mechanism. The developed method was successfully applied in the determination of TAR in different food samples, and this work may be promising for TAR analysis in real samples with rapid, simple quantification.

REFERENCES

1. Baytak A K, Akbas E, Aslanoglu M. A novel voltammetric platform based on dysprosium oxide for the sensitive determination of sunset yellow in the presence of tartrazine [J]. Analytica Chimica Acta, 2019 ; 1087: 93-103.
2. Karimi, Mohammad, Ali. Graphitic Carbon Nitride as a New Sensitive Material for Electrochemical Determination of Trace Amounts of Tartrazine in Food Samples [J]. Food Analytical Methods, 2018 ; 11(10): 2907-2915.
3. Ghalwa N A, Saadeh S M, Harazeen] H E. Development of novel potentiometric sensors for determination of tartrazine dye concentration in foodstuff products [J]. Food Chemistry, 2013 ; 138(1): 126-132.
4. Gan T, Sun J Y, Meng W. Electrochemical sensor based on graphene and mesoporous TiO2 for the simultaneous determination of trace colourants in food [J]. Food Chemistry, 2013 ; 141(4): 3731-3737.
5. Gomez M, Arancibia V, Rojas C. Adsorptive Stripping Voltammetric Determination of Tartrazine and Sunset Yellow in Gelatins and Soft Drink Powder in the presence of Cetylpyridinium Bromide [J]. International Journal of Electrochemical Science, 2012 ; 7(8): 7493-7502.
6. Authority E. Scientific Opinion on the re-evaluation Tartrazine (E 102) [J]. Efsa Journal, 2009 ; 7(11): 1331.
7. Huang Y M, Lai P N, Hsu C L. Surface oxygen plasma modification of screen-printed carbon electrode for quantitative determination of sunset yellow and tartrazine in foods [J]. European Food Research and Technology, 2022 ; 248(3): 881-892.
8. Chen D M, Wu M R, Xie S Y. Determination of Tartrazine, Lutein, Capsanthin, Canthaxanthin and beta-Carotene in Animal-Derived Foods and Feeds by HPLC Method [J]. Journal of Chromatographic Science, 2019 ; 57(5): 462-468.
9. Al Shamari Y M G, Wabaidur S M, Alwarthan A A. Corncob Waste Based Adsorbent for Solid Phase Extraction of Tartrazine in Carbonated Drinks and Analytical Method using Ultra Performance Liquid Chromatography-Mass Spectrometry [J]. Current Analytical Chemistry, 2020 ; 16(7): 924-932.
10. Li K F, Xia Y H, Ma G L. New LC-MS/MS Method for the Analysis of Allura Red Level in Takeaway Chinese Dishes and Urine of an Adult Chinese Population [J]. Journal of Agricultural and Food Chemistry, 2017 ; 65(12): 2588-2593.
11. Sahraei R, Farmany A, Mortazavi S S. A nanosilver-based spectrophotometry method for sensitive determination of tartrazine in food sample [J]. Food Chemistry, 2013 ; 138(2-3): 1239-1242.
12. Sakthivel M, Sivakumar M, Chen S M. Electrochemical synthesis of poly(3,4-ethylenedioxythiophene) on terbium hexacyanoferrate for sensitive determination of tartrazine [J]. Sensors and Actuators B-Chemical, 2018 ; 256: 195-203.
13. Dorraji P S, Jalali F. Electrochemical fabrication of a novel ZnO/cysteic acid nanocomposite modified electrode and its application to simultaneous determination of sunset yellow and tartrazine [J]. Food Chemistry, 2017 ; 227: 73-77.
14. Wang Y, Mu Y X, Hu J. Rapid, one-pot, protein-mediated green synthesis of water-soluble fluorescent nickel nanoclusters for sensitive and selective detection of tartrazine [J]. Spectrochimica Acta Part a-Molecular and Biomolecular Spectroscopy, 2019 ; 214: 445-450.
15. Yang X P, Luo N, Tan Z J. A Fluorescence Probe for Tartrazine Detection in Foodstuff Samples Based on

Fluorescence Resonance Energy Transfer [J]. Food Analytical Methods, 2017 ; 10(5): 1308-1316.

16. Zhang J L, Chen H A, Xu K D. Current Progress of Ratiometric Fluorescence Sensors Based on Carbon Dots in Foodborne Contaminant Detection [J]. Biosensors-Basel, 2023 ; 13(2): 233.
17. Han Y, Yang W X, Luo X L. Carbon dots based ratiometric fluorescent sensing platform for food safety [J]. Critical Reviews in Food Science and Nutrition, 2022 ; 62(1): 244-260.
18. Xiang G, Fan H, Zhang H. Carbon dot doped silica nanoparticles as fluorescent probe for determination of bromate in drinking water samples [J]. Canadian Journal of Chemistry, 2017 ; 96(1): 24-29.
19. Yuan L, Jiang L, Liu Z. Selective and sensitive simultaneous detection of tartrazine and Hg2+ based on N-doped yellow-green fluorescent carbon dots [J]. Dyes and Pigments, 2023 ; 209: 110893.
20. John B K, Mathew S, John N. Hydrothermal synthesis of N,S-doped carbon quantum dots as a dual mode sensor for azo dye tartrazine and fluorescent ink applications [J]. Journal of Photochemistry and Photobiology A: Chemistry, 2023 ; 436: 114386.
21. Li Q H, Du H Y, Li J R. Sulfur-rich carbon quantum dots based on Alternanthera philoxeroides and thiourea for the detection of tartrazine [J]. Journal of Materials Science-Materials in Electronics, 2022 ; 33(16): 12808-12818.
22. Jiang L, Yuan L, Liu Z. Facile hydrothermal synthesis and purification of fluorescent carbon dots for food colorant tartrazine detection based on a dual-mode nanosensor [J]. Analytical Methods, 2022 ; 14(41): 4127-4132.
23. Liu L, Sun H, Xiao L. Development of a highly sensitive fluorescence method for tartrazine determination in food matrices based on carbon dots [J]. Anal Bioanal Chem, 2021 ; 413(8): 2275-2275.
24. Yang X, Xu J, Luo N. N,Cl co-doped fluorescent carbon dots as nanoprobe for detection of tartrazine in beverages [J]. Food Chem, 2020 ; 310: 125832.
25. Thulasi S, Kathiravan A, Asha Jhonsi M. Fluorescent Carbon Dots Derived from Vehicle Exhaust Soot and Sensing of Tartrazine in Soft Drinks [J]. ACS Omega, 2020 ; 5(12): 7025-7031.
26. Ghereghlou M, Esmaeili A A, Darroudi M. Green Synthesis of Fluorescent Carbon Dots from Elaeagnus angustifolia and its Application as Tartrazine Sensor [J]. J Fluoresc, 2020 ; 31(1): 185-193.
27. Li Y P, Jia Y, Zeng Q. A multifunctional sensor for selective and sensitive detection of vitamin B12 and tartrazine by Forster resonance energy transfer [J]. Spectrochimica Acta Part a-Molecular and Biomolecular Spectroscopy, 2019 ; 211: 178-188.
28. Chatzimitakos T, Kasouni A, Sygellou L. Two of a kind but different: Luminescent carbon quantum dots from Citrus peels for iron and tartrazine sensing and cell imaging [J]. Talanta, 2017 ; 175: 305-312.
29. Xie Y T, Zheng J X, Wang Y L. One-step hydrothermal synthesis of fluorescence carbon quantum dots with high product yield and quantum yield [J]. Nanotechnology, 2019 ; 30(8): 085406.
30. Li B, Xiang G, Huang G. Self-exothermic reaction assisted green synthesis of carbon dots for the detection of para-nitrophenol and β-glucosidase activity [J]. Arabian Journal of Chemistry, 2023 ; 16(7): 104820.
31. Su K, Xiang G, Jin X. Gram-scale synthesis of nitrogen-doped carbon dots from locusts for selective determination of sunset yellow in food samples [J]. Luminescence : the journal of biological and chemical luminescence, 2021 ; 31(1): 118-126.
32. Alam A M, Park B Y, Ghouri Z K. Synthesis of carbon quantum dots from cabbage with down- and up-conversion photoluminescence properties: excellent imaging agent for biomedical applications [J]. Green Chemistry, 2015 ; 17(7): 3791-3797.

33. Zhang G-Q, Shi Y-H, Wu W. A fluorescent carbon dots synthesized at room temperature for automatic determination of nitrite in Sichuan pickles [J]. Spectrochimica Acta Part a-Molecular and Biomolecular Spectroscopy, 2023； 286: 122025.
34. Zhu J T, Chu H Y, Shen J W. Nitrogen and fluorine co-doped green fluorescence carbon dots as a label-free probe for determination of cytochrome c in serum and temperature sensing [J]. Journal of Colloid and Interface Science, 2021； 586: 683-691.
35. Huang X S, Liu Z K, Huang Y Q. One-pot room temperature synthesis of orange-emitting carbon dots for highly-sensitive vitamin B12 sensing [J]. Spectrochimica Acta Part a-Molecular and Biomolecular Spectroscopy, 2022； 276: 121239.
36. Midya L, Sarkar A N, Das R. Crosslinked chitosan embedded TiO2 NPs and carbon dots-based nanocomposite: An excellent photocatalyst under sunlight irradiation [J]. Int J Biol Macromol, 2020； 164: 3676-3686.
37. Deng X, Wu D. Highly sensitive photoluminescence energy transfer detection for 2,4,6-trinitrophenol using photoluminescent carbon nanodots [J]. Rsc Advances, 2014； 4(79): 42066-42070.
38. Chen Y Q, Lian H Z, Wei Y. Concentration-induced multi-colored emissions in carbon dots: origination from triple fluorescent centers [J]. Nanoscale, 2018； 10(14): 6734-6743.
39. Fan H H, Xiang G Q, Wang Y L. Manganese-doped carbon quantum dots-based fluorescent probe for selective and sensitive sensing of 2,4,6-trinitrophenol via an inner filtering effect [J]. Spectrochimica Acta Part a-Molecular and Biomolecular Spectroscopy, 2018； 205: 221-226.
40. Liu H, Xu C, Bai Y. Interaction between fluorescein isothiocyanate and carbon dots: Inner filter effect and fluorescence resonance energy transfer [J]. Spectrochimica Acta Part a-Molecular and Biomolecular Spectroscopy, 2017； 171: 311-316.
41. Gu Q, Kenny J E. Improvement of Inner Filter Effect Correction Based on Determination of Effective Geometric Parameters Using a Conventional Fluorimeter [J]. Analytical Chemistry, 2009； 81(1): 420-426.
42. Xu H, Yang X P, Li G. Green Synthesis of Fluorescent Carbon Dots for Selective Detection of Tartrazine in Food Samples [J]. Journal of Agricultural and Food Chemistry, 2015； 63(30): 6707-6714.
43. Gumrukcuoglu A, Basoglu A, Kolayli S. Highly sensitive fluorometric method based on nitrogen-doped carbon dot clusters for tartrazine determination in cookies samples [J]. Turkish Journal of Chemistry, 2020； 44(1): 99-+.